J Stat Phys (2009) 134: 337–364
DOI 10.1007/s10955-009-9679-3

Statistical Mechanics of Complex Systems for Pattern Identification

Shalabh Gupta · Asok Ray

Received: 27 August 2008 / Accepted: 8 January 2009 / Published online: 24 January 2009

Abstract This paper presents a statistical mechanics concept for identification of behavioral patterns in complex systems based on measurements (e.g., time series data) of macroscopically observable parameters and their operational characteristics. The tools of statistical mechanics, which provide a link between the microscopic (i.e., detailed) and macroscopic (i.e., aggregated) properties of a complex system are used to capture the emerging information and to identify the quasi-stationary evolution of behavioral patterns. The underlying theory is built upon *thermodynamic formalism* of symbol sequences in the setting of a *generalized Ising model* (GIM) of lattice-spin systems. In this context, transfer matrix analysis facilitates construction of pattern vectors from observed sequences. The proposed concept is experimentally validated on a richly instrumented laboratory apparatus that is operated under oscillating load for identification of evolving microstructural changes in polycrystalline alloys.

Keywords Complex systems · Generalized Ising model · Lattice spin systems · Thermodynamic formalism · Pattern analysis

Nomenclature

$\mathcal{B}$	Block space of all n-blocks for all $n \in \mathbb{N}$
$\mathcal{B}^{(n)}$	n-block space
$\lvert\mathcal{B}^{(n)}\rvert$	Size of n-block space
$d(\bullet, \star)$	Distance between pattern vectors $\bullet$ and $\star$

This work has been supported in part by the U.S. Army Research Office (ARO) under Grant No. W911NF-07-1-0376, by NASA under Cooperative Agreement No. NNX07AK49A, and by the U.S. Office of Naval Research (ONR) under Grant No. N00014-08-1-0380. Any opinions, findings and conclusions or recommendations expressed in this publication are those of the authors and do not necessarily reflect the views of the sponsoring agencies.

S. Gupta · A. Ray (✉)
The Pennsylvania State University, University Park, PA 16802, USA
e-mail: axr2@psu.edu

S. Gupta
e-mail: szg107@psu.edu

$\mathcal{E}_{\theta\varphi}$	Interaction energy of transition from q_θ to q_φ
$\mathcal{F}_{\theta\varphi}$	General Interaction energy function for transition from q_θ to q_φ
$\mathcal{H}$	Hamiltonian for a dynamical system
ℓ	Number of block symbol transformations of a symbol sequence
$\mathcal{M}$	Mapping from the phase space to the symbol space
$N(\bullet)$	Frequency count of $\bullet$
n	Length of a symbol sequence
$\mathcal{P}(\bullet)$	Probability of an event $\bullet$
$\mathbf{p}^{s_j}$	Pattern vector at slow-time epoch t_{s_j}
$\mathbf{p}^{ref}$	Pattern vector at the reference condition
$\mathcal{Q}$	Set of ϵ-equivalence classes
$\|\mathcal{Q}\|$	Number of ϵ-equivalence classes
$\mathcal{Q}^{[\ell]}$	Set of ϵ-equivalence classes for a symbol sequence generated after ℓ block symbol transformations
q_θ	An ϵ-equivalence class
$q_\theta^{[\ell]}$	An ϵ-equivalence class for a symbol sequence generated after ℓ block symbol transformations
$q_{\theta_k}^{[\ell]}$	An ϵ-equivalence class observed at time index k
r	Order of the Markov process
S	Shannon entropy of the symbol sequence
$\mathcal{S}$	Spin alphabet
$\|\mathcal{S}\|$	Spin alphabet size
s_k	Spin at lattice site k
$\mathcal{T}$	Transfer matrix
T	Temperature of a dynamical system
$\mathcal{T}^{s_j}$	Transfer matrix generated at slow-time epoch t_{s_j}
$\mathcal{T}^{ref}$	Transfer matrix generated at reference, i.e., the nominal condition
t_{s_j}	Slow time epoch s_j
$\mathcal{U}^{s_j}$	Pattern matrix derived from transfer matrix at slow-time epoch t_{s_j}
$\mathcal{U}^{ref}$	Pattern matrix generated at reference, i.e., the nominal condition
$\mathbf{u}$	Input excitation vector of a dynamical system
$\mathbf{x}$	State vector in the phase space
$\mathbf{x}_j$	State vector at (fast) time instant j
$\mathbf{x}_0$	Initial state vector
$\mathbf{y}$	Measurement vector
$\mathcal{Z}$	Partition function for a dynamical system
β	Inverse of a temperature-like parameter for a dynamical system
$\boldsymbol{\gamma}$	Measurement model
δ	Transition mapping from equivalence class to another
η	Tolerance for the stopping rule
$\boldsymbol{\eta}$	(Non-additive) process noise
$\boldsymbol{\varphi}$	Map of a dynamical system
μ	Macroscopic parameter indicating deviation from the reference condition
$\boldsymbol{\nu}$	(Additive) measurement noise
Ξ	A compact region in the phase space
$\boldsymbol{\xi}$	A set of partitioning cells of Ξ
π	Entropy rate of a symbolic stochastic process
Σ	Symbol alphabet that labels the partition segments
$\|\Sigma\|$	Alphabet size

$\Sigma^{[i]}$	Symbol alphabet used at ith block symbol transformation
$\lvert\Sigma^{[i]}\rvert$	Size of $\Sigma^{[i]}$
σ_k	A symbol at (fast scale) time index k
$\overleftarrow{\sigma}_k^{(n)}$	n-block ending at current time index k
$\Phi_{\theta\varphi}$	Strength classifier for transition from q_θ to q_φ
χ	The magnitude of shift of a window on a symbol sequence

1 Introduction

Statistical mechanics provides an elaborate explanation of emergence of macroscopic behavior in a complex system, where the complexity accrues from the activities of its microscopic constituents. The macroscopic and microscopic behavior could be linked by statistical patterns that represent the probability distribution of microstates [1]. The concepts of statistical mechanics, which were originally developed to study the collective properties of physical systems (e.g., solids, liquids, and gases), have been extensively applied to investigate a diverse range of systems including chemical & biological (e.g., colloids, emulsions, liquid crystals, complex fluids, polymers, bio-polymers and cellular structures) [2–4], economical and sociological [5, 6], ecological [7], and a variety of network systems [8–10]. The fundamental principles of equilibrium statistical mechanics are used to investigate stationary and quasi-stationary behavior of complex systems. This discipline is known as *thermodynamic formalism of complex systems* [11–13] in the applied physics literature. Applications of statistical mechanics have been largely successful in the above studies, because it is possible to identify a hierarchical structure based on the order and complexity associated with each level of the hierarchy. Usually the top (i.e., macroscopic) level represents relatively simple and aggregated behavior that emerges from the underlying complex behavior at the lower (i.e., microscopic) level(s). In general, this hierarchy may consist of a multi-tier structure with each tier having a different level of complexity. For example, in nuclear reactor systems, complexity varies on a multi-scale structure due to wide ranges of length, time and energy scales. Since a hierarchical organization of complexity is commonly exhibited by many natural and human-engineered complex systems, statistical mechanics serves as an ideal conceptual platform to study these systems [12].

A critical issue in the theory of complex dynamical systems is to construct a mathematical model to capture the essentials of the underlying process dynamics. Such a model must be computationally tractable and preferably have a closed form solution. However, commonly known dynamical systems (e.g., human-engineered complex systems) are often surmounted by different problems that restrict applications of the fundamental laws of physics to achieve the required modeling accuracy and precision. These problems include: (i) high dimensionality of the phase space, (ii) nonlinear and non-stationary (possibly chaotic) dynamics [14], (iii) parametric or non-parametric uncertainties, (iv) random intrinsic or exogenous excitations, and (v) environmental disturbances. The modeling efforts are further restricted if the operating conditions are extended beyond the nominal operational envelopes due to transient and emergency situations or due to natural evolution of anomalies [15]. (Note: an anomaly, *benign or malignant*, in a dynamical system is defined as a deviation of its current behavioral pattern from its nominal behavior pattern.) For example, no existing model in the current state-of-the-art can capture the behavior of fatigue damage evolution in polycrystalline alloys at the grain level [16] by solely relying on the basic fundamentals of physics. Furthermore, the available models may not be able to provide a closed form solution in general;

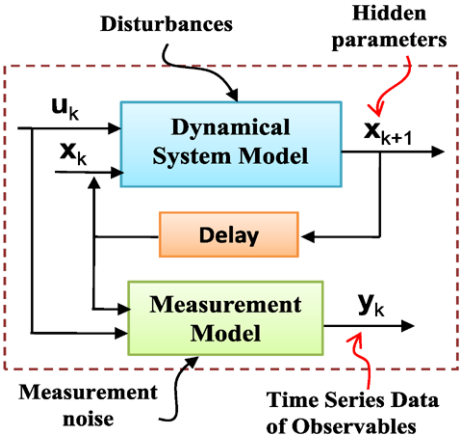

Fig. 1 Measurement of a physical process by a set of observable parameters

therefore, the model outputs have to be generated via numerical techniques (e.g., nonlinear finite-element methods), which are often computationally expensive and infeasible for real-time applications.

The above discussion evinces the need for alternative means of information extraction to capture the underlying dynamics of complex systems. Instead of solely relying on approximate mathematical models (possibly with no established error bounds), the information sources must include adequate sensor data as time series of the critical observable parameters and their operational characteristics. Nevertheless, the sensor information should be augmented, as necessary, by the information derived from the auxiliary analytical models of the system if such models are available. Based on the information ensemble (e.g., combined sensor-based and model-based), the problem is formulated as *observation-based estimation* of the underlying dynamics of a complex system, as depicted in Fig. 1. This concept requires identification of macroscopic properties from the underlying behavior exhibited by the observed time series data [17]. To achieve this goal, the information contained in time series data is compressed in terms of behavioral patterns that are represented by statistical distributions of critical parameters of the system. The resulting macroscopic information, derived from these behavioral patterns, could be used for performance and degradation monitoring, and decision & control under adverse conditions and emergency situations. Technical literature has shown conceptual similarities between the disciplines of complex dynamical systems and statistical mechanics [11–13, 18, 19], which suggest that the theory of thermodynamic formalism has the potential for extraction of the macroscopic properties of a dynamical system from the observed information ensemble [20, 21].

The primary objective of this paper is to formulate a methodology, based on the principles of statistical mechanics, to construct behavioral patterns from the observed sensor data that represent the evolving characteristics of the underlying process dynamics of the system. As stated earlier, in absence of appropriate mathematical models, the concept of behavioral pattern identification in complex systems is based on measurements (i.e., time series data) of observable parameters. The methodology presented in this paper is built upon the principles of lattice-spin systems in the setting of symbolic representations (i.e., symbol sequences) of the underlying process dynamics. Such symbolic representations are generated by appropriate partitioning of the observed time series data [22, 23] and are analogous in structure to lattice-spin systems [1, 13, 24]. The construction of an Ising model from symbol sequences facilitates formulation of a transfer matrix that is a Perron-Frobenius operator [13]. Subsequently, the pattern vector is derived from the transfer matrix, as the sum-normalized left

eigenvector of the unity eigenvalue, to represent the underlying process dynamics of the system. In this context, this paper formulates the pattern identification problem using the tools of lattice spin systems to capture the stationary and quasi-statically evolving behavior of the system. In this paper, the thermodynamic formalism of symbol sequences is based on the generalized Ising model (GIM), i.e., the Potts model [25–28], that describes a lattice spin system for a spin alphabet $\mathcal{S}$ with $|\mathcal{S}| \geq 2$. (Note: The Potts model is a generalization of the Ising model [29, 30] that is restricted to the binary alphabet, i.e., $|\mathcal{S}| = 2$).

The paper presents analytical relationships between the concepts of *statistical mechanics* and *symbolic dynamics* and applies these multidisciplinary concepts to identify behavioral patterns of *complex dynamical systems*. This paper addresses the needs of diverse research communities in the disciplines of applied physics and related sciences, and has, therefore, succinctly presented some of the fundamental details for self sufficiency and completeness. The underlying theories, presented in this paper, have been experimentally validated on a laboratory apparatus for early detection of gradually evolving microstructural damage in polycrystalline alloys under oscillating load. Time series data have been collected from ultrasonic sensors on this apparatus. Based on these data sets, efficacy of pattern identification method has been demonstrated in terms of early detection of behavioral pattern changes due to (possible) evolution of anomalies. From these perspectives, major contributions of the paper are delineated below:

- Analytical formulation of an analogy between the concepts of symbolic dynamics and lattice spin systems.
- Generalized Ising model formalism for an r^{th} $(r \geq 1)$ order Markov symbol sequence derived from the observed data set.
- Construction of pattern identification algorithms based on transfer matrix analysis of generalized Ising models.
- Generalization of the pattern identification algorithms to include coarser representations of dynamical system via block symbol transformations of the symbol sequence.
- Experimental validation of pertinent theoretical results on a laboratory apparatus.

The paper is organized in five sections, including the present section, and two appendices. Section 2 presents a statistical mechanics perspective of dynamical systems. Section 3 briefly describes the basic concepts of symbolic dynamics and presents an analogy between a lattice spin system and a symbolic representation of a statistically stationary dynamical system. In this section, a generalized Ising model (GIM) formalism of symbol sequences is presented and the transfer matrix method is adopted for pattern identification. Section 4 provides pertinent experimental results for validation of the concepts on a laboratory apparatus. The paper is concluded in Sect. 5 along with recommendations for future research. Appendix A presents the concepts of sliding block codes and Appendix B presents a stopping rule to determine the lengths of symbol sequences as needed for generation of transfer matrices.

2 A Statistical Mechanics Perspective of Complex Dynamical Systems

As described in the previous section, this paper incorporates the principles of statistical mechanics into the theory of complex dynamical systems for pattern identification. Before embarking on the details, the following two issues are addressed:

Issue #1: Description of microscopic and macroscopic behaviors in dynamical systems in the setting of *Thermodynamic Formalism*.

Issue #2: Establishment of the link between microscopic and macroscopic behaviors in dynamical systems by using the tools of statistical mechanics.

To address the above issues, let us consider a typical dynamical system whose map is given by:

$$\mathbf{x}_{k+1} = \boldsymbol{\varphi}(\mathbf{x}_k, \mathbf{u}_k, \boldsymbol{\eta}_k); \qquad \mathbf{y}_k = \boldsymbol{\gamma}(\mathbf{x}_k, \mathbf{u}_k) + \boldsymbol{\upsilon}_k \tag{1}$$

where k is the discrete time index; $\boldsymbol{\varphi}$ describes the time evolution of state trajectories and the structure of $\boldsymbol{\varphi}$ may slowly vary with time; $\boldsymbol{\gamma}$ represents the measurement model; $\mathbf{x}$ is the state vector in the phase space; $\mathbf{u}$ is the input excitation vector; $\mathbf{y}$ is the measurement vector; $\boldsymbol{\eta}$ is the (possibly non-additive) process noise; and $\boldsymbol{\upsilon}$ is the additive measurement noise. Evolution of the dynamical system generates a time series data set $\{\ldots, \mathbf{x}_k, \mathbf{x}_{k-1}, \ldots, \mathbf{x}_0\}$ of the state vector $\mathbf{x}$ starting from an initial point $\mathbf{x}_0$. As discussed earlier in Sect. 1, the state vector $\mathbf{x}$ is usually hidden and the map $\boldsymbol{\varphi}$ is generally difficult to determine, especially for off-nominal or anomalous systems. Therefore, the measurement set $\mathbb{Y} = \{\ldots, \mathbf{y}_k, \mathbf{y}_{k-1}, \ldots, \mathbf{y}_0\}$ of selected observable outputs (e.g., sensor data) are used to provide insights into the necessary details of the system, as illustrated in Fig. 1. Having said that, the concept of two-time-scales in the analysis of dynamical systems need to be discussed.

Definition 2.1 The *fast scale* is defined to be the time scale over which the behavior of the dynamical system is assumed to remain shift-invariant, i.e., the process has stationary dynamics.

Definition 2.2 The *slow scale* is defined to be the time scale over which the system may exhibit non-stationary dynamics.

In view of Definition 2.1, variations in the internal dynamics of the system are assumed to be negligible on the fast scale. Since stationarity is assumed to be preserved on the fast scale, it is best suited for acquisition of time series data from sensor and/or analytical measurements (i.e., information derived from analytical models). In view of Definition 2.2, an observable non-stationary behavior can be associated with the gradual evolution of the system possibly due to gradual development of anomalies. In general, a long time span in the fast scale is a tiny (i.e., possibly several orders of magnitude smaller) interval in the slow scale. For example, evolution of fatigue damage in polycrystalline alloys may cause a detectable change in the system dynamics on the slow scale (possibly in the order of hours or months) while this damage behavior is essentially invariant on the fast scale (approximately in the order of seconds or minutes). Nevertheless, the notion of fast and slow scales is dependent on the specific application, loading conditions and operating environment. As such, with the objective of monitoring the changes in a dynamical system, acquisition of time series data is performed on the fast scale at different slow-time epochs. A pictorial view of the two-time scales concept is presented in Fig. 2.

The notion of fast and slow scales can also be extended to multidimensional data sets (e.g., a two dimensional image data). Here, the notion of time is replaced by space. In such cases, the fast scale is defined as the scale over which the space data represents the local fluctuations in the region under observation. The statistical features of spatial fluctuations in this local region remain invariant. On the other hand, the slow scale is defined to be the scale over which the statistical features of spatial fluctuations may change. For example, in a two-dimensional image of a natural geographical location, one natural feature (e.g., densely populated tall trees) might be the characteristic of a local space that changes to another

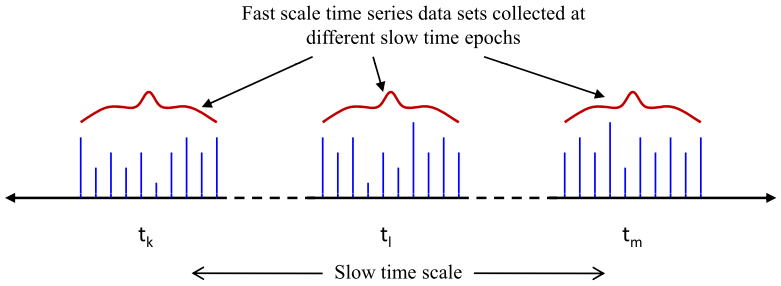

Fig. 2 Pictorial view of two time scales: (i) *Slow scale* of system evolution and (ii) *Fast scale* for data acquisition and signal conditioning

natural feature (e.g., sporadic short bushes) over a slow scale in the image. This concept of fast and slow scales is important in characterizing the local and global dynamics of a system in time or space or both. In the sequel, observed data are referred to as time series for convenience.

Remark 2.1 Steady state behavior of the dynamical system under consideration is assumed to be stationary on the fast scale, which implies that the time series data obey the laws of equilibrium statistical mechanics. In contrast, on the slow scale, the dynamical system may be in a quasi-static equilibrium condition or in a non-equilibrium condition between two slow-time epochs, depending on its evolution. In essence, the dynamical system may deviate from the equilibrium at a particular slow-time epoch and attain another equilibrium under evolving dynamics at a subsequent slow-time epoch.

Time series data collected on the fast scale contains microscopic (i.e., detailed) information at each instant. The amount and quality of information in the time series data may depend on the sensor and/or analytical measurements. As such, each data point in the time series carries microscopic details that are rather irrelevant for understanding the behavior patterns of a dynamical system. However, the data sequence as a whole represents macroscopic (i.e. aggregated) behavior of the dynamical system at the respective slow-time epoch. The time series may contain several bursts of fast-scale data at a slow-time epoch. It is reasonable to assume ergodicity [13] on the fast scale, i.e., convergence of the time average to the ensemble average. In this context, the two issues, stated at the beginning of this section, are addressed as follows:

Issue #1: While each data point of the fast scale time series contains the microscopic details, the information derived from a time series, represents the ensemble average, i.e., the macroscopic behavior of the dynamical system, at a specific slow-time epoch. The terms "microscopic" and "macroscopic" are understood as detailed behavior and aggregated behavior of the dynamical system, respectively.

Issue #2: In statistical mechanics, the macroscopic behavior of a system is represented by a few intensive parameters (e.g., pressure and temperature) that are derived from the probability distributions of the microstates [1]. These probability distributions are postulated based on the microscopic activities of individual particles and their (possible) mutual interactions. In the inverse approach of statistical mechanics, the objective is to estimate macroscopic model parameters of the system based on the microscopic laws expressed by probability distributions over microstates.

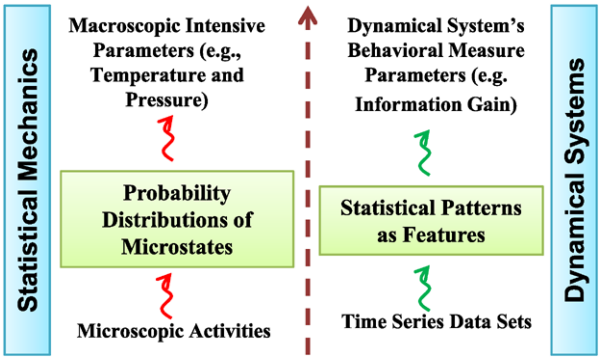

Fig. 3 Analogy between the concepts of statistical mechanics and dynamical systems

In general, mathematical models of complex dynamical systems might be difficult (and often impossible) to identify, as discussed in Sect. 1. Therefore, an alternative is to identify statistical patterns of the evolving dynamics based on observed time series data from available sensors. The objective is to derive macroscopic (i.e., aggregated) behavior from the statistical patterns (e.g., probability distributions and statistical correlations) that are generated from time series of observables (i.e., sensor outputs and/or analytical measurements [13, 15]). These statistical patterns provide the required link between the microscopic and macroscopic behavior of a complex dynamical system, as illustrated in Fig. 3.

There are several ways of constructing statistical patterns. In general, the link between microscopic and macroscopic behavior in dynamical systems need not even be statistical in nature. The macroscopic information could be derived by using several different pattern identification algorithms [31]. This paper presents a statistical method of constructing the link between microscopic and macroscopic behavior of dynamical systems by drawing an analogy between the concepts of symbolic dynamics and lattice spin systems. This thermodynamic formalism is insightful for studying the properties of aggregated behavior that arises from the underlying complexity in complex systems.

3 Symbolic Dynamic Encoding and Thermodynamic Formalism

The tools of symbolic dynamics are often used to study the behavior of complex dynamical systems [15, 22, 32–34]. In symbolic dynamics, the phase space of a dynamical system is partitioned for representing its state trajectory with a symbol sequence. Let $\Xi \subset \mathbb{R}^n$ be a compact (i.e., closed and bounded) region in the (n-dimensional) phase space within which the (statistically stationary) trajectory is circumscribed under a specific exogenous stimulus. Encoding of Ξ is accomplished by introducing a partition $\{\xi_1, \ldots, \xi_{|\Sigma|}\}$ consisting of $|\Sigma|$ mutually exclusive (i.e., $\xi_j \cap \xi_k = \emptyset \; \forall j \neq k$), and exhaustive (i.e., $\bigcup_{j=1}^{|\Sigma|} \xi_j = \Xi$) cells, where Σ is the *symbol alphabet* that labels the partition segments (Note: $2 \leq |\Sigma| < \infty$). As the system evolves in time (fast scale), the state trajectory travels through or touches various cells in its phase space; accordingly the corresponding symbol is assigned to each point $\mathbf{x}_i$ of the trajectory as defined by the mapping $\mathcal{M} : \Xi \to \Sigma$. Therefore, a symbol sequence is generated from an initial state $\mathbf{x}_0 \in \Xi$, such that:

$$\cdots \sigma_k \cdots \sigma_1 \sigma_0 \leftarrowtail \mathbf{x}_0 \tag{2}$$

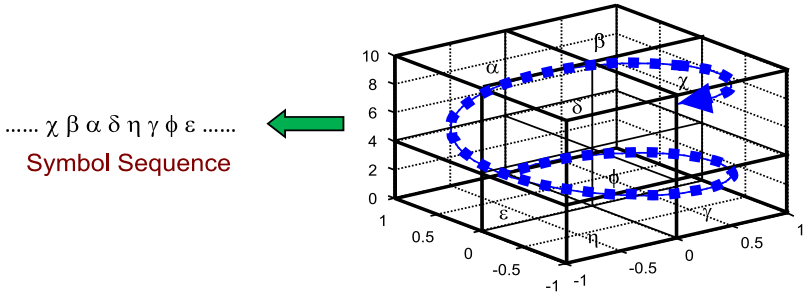

Fig. 4 Concept of phase space partitioning for symbol sequence generation

where $\sigma_k \triangleq \mathcal{M}(\mathbf{x}_k)$ is the symbol generated at the (fast scale) instant k. (Note: the direction of forward time has been chosen to be towards the left in (2) for convenience.)

The mapping in (2) is called *symbolic dynamics* as it attributes a legal (i.e., physically admissible) symbol sequence to the system dynamics starting from an initial state. (Note: The partition is called a generating partition of the phase space Ξ if every legal symbol sequence uniquely determines a specific initial condition $\mathbf{x}_0$, i.e., every symbolic orbit uniquely identifies one continuous space orbit.) The pictorial display in Fig. 4 elucidates the concept of partitioning a compact region of the phase space and mapping from the partitioned space into the symbol alphabet.

3.1 Generation of a Symbol Sequence from Observed Data

A crucial step in symbolic dynamic encoding is partitioning of the phase space for symbol sequence generation. Several partitioning techniques have been reported in literature to address this issue [13]. Although the theory of phase-space partitioning is well developed for one-dimensional mappings, few results are known for two and higher dimensional systems. For example, the widely used method of symbolic false nearest-neighbors (*SFNN*) [23] may become computation-intensive if the dimension of the phase space is large or if the available data are noise-corrupted. Furthermore, the state trajectory of the system may be unknown in case of systems for which a model as in (1) is not available.

As an alternative to phase space partitioning, the fast scale time series data set $\mathbb{Y} = \{\ldots, \mathbf{y}_k, \mathbf{y}_{k-1}, \ldots, \mathbf{y}_0\}$ of selected observable outputs (e.g., sensor data) can be directly used for symbolic dynamic encoding. In this regard, several techniques have been reported in literature that suggest appropriate transformation of the signal before employing the partitioning method for symbol generation to retrieve the relevant information from time series data. One such technique is based on wavelet transform [35] of time series data, called the wavelet-space partitioning (*WSP*) [15, 36] that is particularly effective with noisy data from high-dimensional dynamical systems. Another reported technique is analytic-signal-space partitioning (*ASSP*) [37] based on the Hilbert transform of time series data. Details of these partitioning methods are readily available in literature [36, 37] and are not provided in this paper.

The resulting transformed data can be partitioned using different methods. One such method is uniform partitioning into equal sized cells. Other method is based on the principle of maximization of the Shannon entropy [38]:

$$S = -\sum_{i=1}^{|\Sigma|} p_i \log(p_i) \tag{3}$$

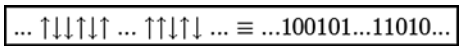

Fig. 5 Equivalence of the one-dimensional structure of Ising model and a symbolic sequence with alphabet set $\Sigma = \{0,1\}$

where p_i is the probability of the ith segment of the partition. Uniform probability distribution is a consequence of *maximum entropy partitioning* that makes the partition coarser in regions of low data density and finer in regions of high data density [36].

3.2 Lattice Spin System Formalism of the Symbol Sequence

The symbolic representation of stationary stochastic time series of observable parameters is constructively similar to the structure of a lattice spin system such that, at an instant k in the fast scale, the observed symbol $\sigma_k \in \Sigma$ is analogous to a spin $s_k \in \mathcal{S}$ at the lattice site k [24] with the constraint that Σ and $\mathcal{S}$ must have the same cardinality. Since both Σ and $\mathcal{S}$ are finite nonempty sets, it implies that $|\Sigma| = |\mathcal{S}|$ and $|\Sigma| \in \mathbb{N}$, where $\mathbb{N}$ is the set of all positive integers. The generalized Ising model (GIM), i.e., the Potts model [25–27], describes a lattice spin system using a spin alphabet $\mathcal{S}$ with $|\mathcal{S}| \geq 2$, whereas the Ising model [29, 30] is restricted to the binary spin alphabet, i.e., $|\mathcal{S}| = 2$. Therefore, the GIM allows for a larger alphabet for partitioning. The equivalence between symbolic representation of a dynamical system and a lattice spin system is illustrated in Fig. 5 for the simplest case of the Ising model with $\mathcal{S} = \{\uparrow, \downarrow\}$, which has one to one correspondence to the symbol sequence generated with $\Sigma = \{0, 1\}$. In general, spin systems can be translated into symbolic stochastic processes and vice versa. Thus, the methods of statistical mechanics are applicable to analysis of chaotic dynamical systems [13].

This section presents construction of an appropriate Hamiltonian in the setting of the generalized Ising model (GIM) of symbol sequences generated from observed time series data [21]. This thermodynamic formalism of dynamical systems enables information extraction in the form of statistical patterns that facilitate robust detection of gradually evolving changes in the underlying process dynamics [15].

3.2.1 Equivalence classes of symbol sequences

Let us introduce the notion of equivalence classes on symbol sequences and the concept of transition energies before constructing the Hamiltonian for a dynamical system. In this regard, the following definitions are introduced.

Definition 3.1 A block is a finite string of symbols over an alphabet. A block of length $n \in \mathbb{N}$ is called an n-block, where $\mathbb{N}$ is the set of all positive integers. An n-block is denoted as $\overleftarrow{\sigma}_k^{(n)} \triangleq \sigma_k \cdots \sigma_{k-n+1}$ that is a symbolic representation of a time series in the fast scale starting at instant $k-n+1$ and ending at instant k. (The direction of arrow indicates forward time.)

Definition 3.2 Let the block space $\mathcal{B}$ be the set of n-blocks over the symbol alphabet Σ for all $n \in \mathbb{N}$. In general, cardinality of $\mathcal{B}$ is $\aleph_0$, which is the same as the cardinality of $\mathbb{N}$; however, some of the blocks may be physically inadmissible. A probability measure space is defined as $(\mathcal{B}, \mathcal{A}, \mathcal{P})$, where $\mathcal{B}$ is the sample space; $\mathcal{A}$ is the event space that is a σ-algebra [39] of $\mathcal{B}$ and contains the singleton sets of all physically admissible blocks; and $\mathcal{P}$ is the probability measure such that $\mathcal{P} : \mathcal{A} \rightarrow [0, 1]$. The probability measure of each of the

physically inadmissible blocks is assigned to be zero. (The blocks with zero probability are not included in the analysis that follows.)

Definition 3.3 For a given $r \in \mathbb{N}$, a symbolic sequence is called r-Markov if the conditional probability of each symbol, in the alphabet Σ, depends only on the previous (at most) r symbols in the following sense:

$$\mathcal{P}(\sigma_k|\sigma_{k-1}\sigma_{k-2}\cdots\sigma_{k-r}\sigma_{k-r-1}\cdots) = \mathcal{P}(\sigma_k|\sigma_{k-1}\cdots\sigma_{k-r}). \tag{4}$$

Let us define the equivalence classes in the block space $\mathcal{B}$ and show how $\mathcal{B}$ is partitioned under the Markov assumption into a finite set of equivalence classes. Let b_θ and b_φ be two blocks in block space $\mathcal{B}$. [*Notation*: The Greek letter subscripts θ and φ of blocks b_θ and b_φ denote two arbitrary blocks in the block space $\mathcal{B}$. In contrast, the subscripts i and j of symbols σ_i and σ_j denote time instants in the fast scale.]

Definition 3.4 An equivalence class is defined such that $b_\theta \in \mathcal{B}$ and $b_\varphi \in \mathcal{B}$ belong to the same class if the probabilities of their physically admissible transitions are identical in the following sense:

$$\mathcal{P}(b|b_\theta) = \mathcal{P}(b|b_\varphi) > 0 \quad \forall b \in \mathcal{B}. \tag{5}$$

In a statistically stationary dynamical system [13], the probability measure $\mathcal{P}$ is an invariant. Therefore, for an r-Markov symbol sequence, Definitions 3.3 and 3.4 imply that, at any time instant k, a past ℓ-block $\overleftarrow{\sigma}_{k-1}^{(\ell)} \in \mathcal{B}$, for all $\ell \geq r \geq 1$, belongs to the same equivalence class as that of a past s-block $\overleftarrow{\sigma}_{k-1}^{(s)} \in \mathcal{B}$, for all $s \geq r \geq 1$, if both contain the same r-block $\overleftarrow{\sigma}_{k-1}^{(r)} \in \mathcal{B}$ of the most recent r symbols. Now the subspace of $\mathcal{B}$, consisting of all n-blocks with $n \geq r$, is partitioned into a set of finitely many equivalence classes, which is isomorphic to $\mathcal{B}^{(r)} \subset \mathcal{B}$. The set $\mathcal{B}^{(r)}$ is called the r-block space and its members are all possible r-blocks; cardinality of $\mathcal{B}^{(r)}$ is denoted as $|\mathcal{B}^{(r)}| \leq |\Sigma|^r$, where the inequality is a consequence of the fact that some of the r-blocks in $\mathcal{B}^{(r)}$ might be forbidden. Therefore, the number of equivalence classes is at most $|\Sigma^{(r)}|$. In the sequel, we analyze the r-block space $\mathcal{B}^{(r)}$ instead of the entire block space $\mathcal{B}$ based on the assumption that the stationary dynamical system is r-Markov for a given $r \in \mathbb{N}$. Let us now relax the condition in Definition (3.4) by introducing a weaker notion of equivalence called ε-equivalence.

Definition 3.5 An ε-equivalence class is defined such that, for a given $0 < \varepsilon \ll 1$, the partitioning $\mathcal{B}^{(r)}$ is formed in the following sense.

1. Each r-block in $\mathcal{B}^{(r)}$ belongs to one and only one of the ε-equivalence classes.
2. If there are two (or more) r-blocks in an ε-equivalence class $\mathcal{C} \subseteq \mathcal{B}^{(r)}$, then

$$\left|\mathcal{P}(b|b_\theta) - P(b|b_\varphi)\right| < \varepsilon \quad \forall b_\theta, b_\varphi \in \mathcal{C}\ \forall b \in \mathcal{B}^{(r)}. \tag{6}$$

The procedure for selection of such ε-equivalence classes falls in the category of clustering methods that have been extensively studied in the Pattern Classification literature (e.g., see citations in [31]). From the statistical mechanics perspective, clusters of r-blocks as ε-equivalence classes is natural because there are finitely many clearly separated energy bands [1] defined by ε, each of which may contain many r-blocks. Therefore, ε-equivalence classes are formed as clusters of r-blocks, where each element of a cluster falls within an energy band of width ε.

Remark 3.1 A symbol sequence can be transformed via the block symbol transformation (i.e, renormalization) before construction of the ε-equivalence classes. Therefore, in general, the equivalence classes can be defined on a renormalized symbol sequence to generate a coarser representation of the system. See Sect. 3.3 for details.

3.2.2 Thermodynamic Formalism of ε-Equivalence Classes

Let us denote each ε-equivalence class in $\mathcal{B}^{(r)}$ as an *energy state* $q \in \mathcal{Q}$, where $|\mathcal{Q}| \leq |\mathcal{B}^{(r)}| \leq |\Sigma|^r$. For a dynamical system, an observed r-block $\overleftarrow{\sigma}_k^{(r)}$ on a symbol sequence at (fast scale) time k belongs to an ε-equivalence class represented by a state $q \in \mathcal{Q}$, i.e., q is a realization of $\overleftarrow{\sigma}_k^{(r)}$. In other words, an energy state is a realization of an r-block on a symbol sequence. As time evolves on fast scale, the symbol sequence gives rise to different r-blocks and transitions take place from one energy state to another (see Remark 3.2 below).

Definition 3.6 The probability of transition from an energy state $q_\theta \in \mathcal{Q}$ to an energy state $q_\varphi \in \mathcal{Q}$ under a transition $\delta : \mathcal{Q} \times \Sigma \to \mathcal{Q}$ is defined as

$$\mathcal{P}(q_\varphi | q_\theta) = P_r(\sigma \in \Sigma \mid \delta(q_\theta, \sigma) \to q_\varphi); \quad \sum_{\varphi} \mathcal{P}(q_\varphi | q_\theta) = 1. \tag{7}$$

Definition 3.7 The interaction energy of the transition from $q_\theta \in \mathcal{Q}$ to $q_\varphi \in \mathcal{Q}$ is defined in terms of the respective transition probability as

$$\mathcal{E}_{\theta\varphi} \equiv \mathcal{E}(q_\varphi | q_\theta) \triangleq -\ln[\mathcal{P}(q_\varphi | q_\theta)]. \tag{8}$$

The thermodynamic formalism of the interaction energy $\mathcal{E}_{\theta\varphi}$ in Definition 3.7 is as follows:

(i) Interaction energy is always non-negative (i.e., $\mathcal{E}_{\theta\varphi} \geq 0$) because $0 \leq \mathcal{P}(\star|\bullet) \leq 1$, which signifies that the energy equivalence of transition from one ε-equivalence class to other is always greater than or equal to zero.
(ii) State transition that has a lower probability requires relatively larger energy (i.e., less reachable) and transitions that have higher probabilities require relatively smaller energies (i.e., more reachable) from the aspects of statistical mechanics.
(iii) Energy is non-commutative with respect to the interacting states, i.e., $\mathcal{E}_{\theta\varphi} \neq \mathcal{E}_{\varphi\theta}$ for $\theta \neq \varphi$, in general.
(iv) All physically admissible transitions have non-zero probabilities and hence finite energies. In particular, if a transition is certain to happen (i.e., the transition probability is equal to 1, then its energy vanishes (i.e., $\mathcal{E}_{\theta\varphi} = 0$). This implies that such a transition requires no energy.
(v) All physically inadmissible transitions (e.g., transition to a forbidden r-block) have zero probabilities and hence require infinite energies. These transitions are not observed at a particular slow-time epoch and are not included in the analysis. However, they may have non-zero probability of occurrence (with finite energy) at other slow-time epochs. An r-block that is forbidden to appear at a slow-time epoch may appear at another slow-time epoch due to possible changes that might have occurred in the dynamical system. In essence, referring to Fig. 2, the dynamical system could be non-stationary in the slow scale although it is assumed to be quasi-stationary in the fast scale.

The definition of interaction energy in (8) is based on the conditional probability of a symbol block given a past block. Therefore, if two symbol blocks that follow different past blocks have the same conditional probabilities with respect to their own past blocks, then they will have the same interaction energy.

Remark 3.2 A symbol sequence that is structured as a lattice consists of several r-blocks. These blocks are constructed by shifting a window of length r by one symbol at a time. Therefore, as time evolves different blocks (i.e., energy states) appear on the sequence and transitions take place from one block to the other.

3.2.3 General Interaction Energy Functions

In general, the interaction energy between any two energy states (i.e., ε-equivalence classes) $q_\theta \in \mathcal{Q}$ and $q_\varphi \in \mathcal{Q}$ depends on respective state transition probability and also on the strength associated with that transition. This implies that a transition between any two states may have a high probability of occurrence but still have a low significance due to a small interaction strength. On the other hand, a transition may have a low probability but still have a high significance due to a high interaction strength. For pattern identification, it is equivalent to saying that certain transitions are more critical than the others for capturing small changes in the dynamical system. For example, some transitions might occur very frequently (possibly) due to measurement noise and therefore, a low strength to these transitions reduces noise. On the other hand, transitions that occur relatively less frequently might be indicative of an incipient fault in the dynamical system and therefore, a high strength to these transitions enables early detection. Therefore, in general, the interaction energy $\mathcal{F}_{\theta\varphi}$ between any two ε-equivalence classes q_θ and q_φ is defined as

$$\mathcal{F}_{\theta\varphi} \equiv \mathcal{F}(q_\varphi|q_\theta) \triangleq -\ln[\Phi(q_\varphi, q_\theta)\mathcal{P}(q_\varphi|q_\theta)] \tag{9}$$

where $\Phi(\bullet, \star)$ is the interaction strength function, such that $0 \leq \Phi(\bullet, \star) \leq 1$ assigns a strength to a transition from $\star$ to $\bullet$. Since these functions classify the strengths associated with interactions between a pair of ε-equivalence classes, they are termed as *Transition Strength Classifiers*. Transition strengths can be tuned to adjust the sensitivity of pattern identification towards certain transitions and be chosen based on relative significance of possible transitions. Two simple examples of the interaction strength function Φ are presented below.

$$\Phi(q_\varphi, q_\theta) = \frac{|\vartheta_\varphi - \vartheta_\theta|^\alpha}{\sum_{\varphi=1}^{|\mathcal{Q}|} |\vartheta_\varphi - \vartheta_\theta|^\alpha}, \tag{10}$$

$$\Phi(q_\varphi, q_\theta) = \frac{|\vartheta_\varphi \vartheta_\theta|^\alpha}{\sum_{\varphi=1}^{|\mathcal{Q}|} |\vartheta_\varphi \vartheta_\theta|^\alpha} \tag{11}$$

where α is a positive real; and ϑ_φ and ϑ_θ are the non-negative weights associated with energy states q_φ and q_θ, respectively.

3.3 Block Symbol Transformation of the Symbol Sequence

The previous section described the lattice spin system formalism of a symbol sequence using the notion of energy states (i.e., ε-equivalence classes) and the interaction energy between them. This formalism is based on symbol sequences that are generated from an alphabet Σ. The interaction energy is defined between pairs of symbol blocks that appear adjacent

to each other shifted by a single symbol on the symbol sequence. In general, the interactions might have a longer range where the effects of local dynamics could be neglected. Therefore, symbolic dynamic encoding of dynamical systems often includes construction of a new alphabet, called elaborate alphabet [22], from blocks of symbols generated from the original alphabet Σ. This approach is useful when the actual information from the data is concentrated in a relatively low frequency range and the information at higher frequencies are not of significant interest; in other words, this approach is capable of capturing the dynamics of long range interactions. For example, the important characteristics of a low-frequency (i.e., long wavelength) signal might be observed in the correlation between different maxima rather than in the local dynamics around each maximum itself. If the critical properties of a physical process depend on long-wavelength fluctuations [30], then irrelevant degrees of freedom need to be eliminated by coarse graining of the data so that the effects of local dynamics are diminished by averaging.

In statistical mechanics, the idea of *block spin* transformation has been introduced to study the critical properties of Ising models. The block spin transformation is part of a theory called the *Renormalization Group* transformation [40][30]. In block spin transformation of an Ising model, an effective Hamiltonian is constructed using block spins, which is based on interactions between blocks of spins rather than between individual spins. Following this concept in dynamical systems, a set of symbols at local discrete-time indices that form a block, are collectively assigned a new symbol on an elaborate alphabet $\Sigma^{[1]}$, which is called the *block symbol* transformation. The core concept of renormalization is that a block in a long symbol sequence is reduced to a single symbol [41] that is equivalent to coarse-graining in time. This procedure can be repeated for generating several coarser representations of the system.

The renormalization procedure of a symbol sequence consists of the following two steps.

(1) Grouping of symbols to form blocks.
(2) Transformation of blocks to new symbols in the elaborate alphabet, called degeneracy.

The block symbol transformation of a symbol sequence $\overleftarrow{\sigma}_{j}^{(n_0)}$ of length n_0 is represented by the following flow diagram.

$$\begin{array}{ccc} \overleftarrow{\sigma}_{j}^{(n_0)} \rightarrow \overleftarrow{\sigma}_{j}^{(w)} \overleftarrow{\sigma}_{j-\chi}^{(w)} \overleftarrow{\sigma}_{j-2\chi}^{(w)} \cdots \\ \downarrow \\ \overleftarrow{\sigma}_{j'}^{(n_1)} \leftarrow \sigma_{j'} \sigma_{j'-1} \sigma_{j'-2} \cdots \end{array}$$

where j' is the transformed time index such that $j' = j - n(\chi - 1)$; $\overleftarrow{\sigma}_{j'}^{(n_1)}$ is the transformed symbol sequence of length n_1; $\sigma_{j'}$ is a symbol in $\Sigma^{[1]}$; and $1 \leq \chi \leq w$ is the magnitude of shift of a window of size w.

The first step in the renormalization procedure is construction of symbol blocks that can be overlapping or non-overlapping. A block is constructed from a window of length w on a symbol sequence that is shifted by χ symbols at a time to obtain another block of length w. For $1 \leq \chi < w$, the blocks are overlapping and this construction represents a *higher block shift* [22]. For $\chi = w$, the blocks are non-overlapping, and this represents a *higher power shift* [22]. In this case, a window on the symbol sequence is shifted to obtain a new block that has no common elements with the previous block. The size of the window w depends on the range of local interactions, while the magnitude of shift χ depends on the range of interactions between symbol blocks. In general, a renormalized sequence can be constructed from a symbol sequence that is structured as either overlapping or non-overlapping blocks.

The second step assigns a new symbol to each block of length w such that a transformed symbol sequence is generated from an elaborate alphabet $\Sigma^{[1]}$. If $|\Sigma^{[1]}| = |\mathcal{B}^{(w)}| \leq |\Sigma|^w$ is chosen for the above assignment, where $\mathcal{B}^{(w)}$ is the space of w-blocks, then it merely changes the nomenclature while preserving the order of symbols in a block because each block configuration is assigned a different symbol; hence, complexity is not reduced. The new elaborate alphabet should be chosen to achieve a higher level of approximation causing degeneracy. A possible choice is to keep the alphabet size the same as the original one, i.e., $|\Sigma^{[1]}| = |\Sigma|$, and to assign a symbol from $\Sigma^{[1]}$ to a block configuration $b_\theta \in \mathcal{B}^{(w)}$ based on a rule $\mathcal{R} : \mathcal{B}^{(w)} \to \Sigma^{[1]}$ (e.g., a symbol that occurs at the mth position in $b_\theta \in \mathcal{B}^{(w)}$ that is denoted by $[b_\theta]_m$). The advantage of this coarser representation of the system is reduction of the irrelevant local dynamics using a small alphabet size that reduces the number of energy states and the size of the transfer matrix (see Sect. 3.5).

In general, the block symbol transformation can be applied repeatedly any number of times. A new alphabet $\Sigma^{[i]}$ (possibly $\Sigma^{[i]}{=}\Sigma$) is used at any ith transformation, where a sequence $\overleftarrow{\sigma}_{j'}^{(n_\ell)}$ of length n_ℓ is generated after ℓ subsequent transformations. The transformed symbol sequence would have interactions between block symbols that are generated from blocks on the original symbol sequence. These interactions lead to new equivalence classes (see Remark 3.1) and their corresponding interaction energies, where the r-Markov dynamics are assumed over the renormalized sequence. (Note: the value of r may vary over different block symbol transformations.) Let us denote the set of energy states (i.e., ε-equivalence classes) on a sequence, which has been renormalized ℓ times, by $\mathcal{Q}^{[\ell]}$, and the interaction energy (see Sect. 3.2) between a pair of energy states, $q_\theta^{[\ell]} \in \mathcal{Q}^{[\ell]}$ and $q_\varphi^{[\ell]} \in \mathcal{Q}^{[\ell]}$, by $\mathcal{F}_{\theta\varphi}^{[\ell]}$ that has the same structure as in (9). The next section describes construction of a generalized Ising model (GIM) using these energy states and their interactions on a symbol sequence.

3.4 Generalized Ising Model Construction

The local space-time behavior of a thermodynamic system's constituents is described by a Hamiltonian; an analogous approach for dynamical systems is presented here. As stated earlier, it is often infeasible to construct a reliable mathematical model of a complex system. Therefore, a Hamiltonian is constructed from the statistics derived from the observed symbol sequences. Let an n_0-block $\overleftarrow{\sigma}_j^{(n_0)}$ be a symbolic stationary process generated by partitioning the (fast scale) time series data $\mathbb{Y} = \{\mathbf{y}_j, \mathbf{y}_{j-1}, \ldots, \mathbf{y}_{j-n_0+1}\}$ that are observed at a particular slow-time epoch (see Sect. 3.1). Let an n_ℓ-block $\overleftarrow{\sigma}_{j'}^{(n_\ell)}$ be obtained after (possible) block symbol transformations of $\overleftarrow{\sigma}_j^{(n_0)}$. Since stationary (possibly Markov) symbol chains are frequently used to construct statistical models of dynamical systems, the Hamiltonian for the symbol block $\overleftarrow{\sigma}_{j'}^{(n_\ell)} \in \mathcal{B}$ can be expressed as a function of the probability of occurrence of $\overleftarrow{\sigma}_{j'}^{(n_\ell)}$. Let us split the symbol block $\overleftarrow{\sigma}_{j'}^{(n_\ell)} \equiv \sigma_{j'}\sigma_{j'-1}\cdots\sigma_{j'-n}\cdots\sigma_{j'-n_\ell+1}$ into an n-block $\overleftarrow{\sigma}_{j'}^{(n)} \equiv \sigma_{j'}\sigma_{j'-1}\cdots\sigma_{j'-n+1}$ of most recent n symbols and an s-block $\overleftarrow{\sigma}_{j'-n}^{(s)} \equiv \sigma_{j'-n}\sigma_{j'-n-1}\cdots\sigma_{j'-n_\ell+1}$ of the remaining symbols observed in the past, where $s = n_\ell - n$. It is assumed that the probability of n-block $\overleftarrow{\sigma}_{j'}^{(n)} \in \mathcal{B}$ depends on the s-block $\overleftarrow{\sigma}_{j'-n}^{(s)} \in \mathcal{B}$ that has been observed in the past. The Hamiltonian, i.e., total energy associated with a transition from $\overleftarrow{\sigma}_{j'-n}^{(s)}$ to $\overleftarrow{\sigma}_{j'}^{(n)}$, is given as:

$$\mathcal{H} \triangleq -\ln[\mathcal{P}(\overleftarrow{\sigma}_{j'}^{(n)} | \overleftarrow{\sigma}_{j'-n}^{(s)})] \tag{12}$$

where $\mathcal{P}(\star|\bullet)$ is the conditional probability of $\star$ given $\bullet$. (Note: the subscript on σ indicates the most recent fast time index and the superscript indicates length of the symbol sequence).

The total interaction energy depends on the observed configurations of $\overleftarrow{\sigma}_{j'}^{(n)} \in \mathcal{B}$ and $\overleftarrow{\sigma}_{j'-n}^{(s)} \in \mathcal{B}$; however, it is denoted as $\mathcal{H}$ for notational simplicity.

Equation (12) is now restructured as having neighborhood interactions in a generalized Ising model (GIM) under Markovian assumption (see Definition 3.3). Subsequently, the transfer matrix approach [1] is adopted for construction of statistical patterns and evaluation of the macroscopic behavior of the system from the observed symbol sequences. Using the Bayesian chain rule for a Markov process, the transition probability $\mathcal{P}(\overleftarrow{\sigma}_{j'}^{(n)} | \overleftarrow{\sigma}_{j'-n}^{(s)})$ on right hand side of (12) is expressed as:

$$\mathcal{P}(\overleftarrow{\sigma}_{j'}^{(n)} | \overleftarrow{\sigma}_{j'-n}^{(s)}) = \mathcal{P}(\sigma_{j'} | \overleftarrow{\sigma}_{j'-1}^{(n+s-1)}) \mathcal{P}(\sigma_{j'-1} | \overleftarrow{\sigma}_{j'-2}^{(n+s-2)}) \cdots \mathcal{P}(\sigma_{j'-n+1} | \overleftarrow{\sigma}_{j'-n}^{(s)}) \tag{13}$$

$$= \mathcal{P}(\sigma_{j'} | \overleftarrow{\sigma}_{j'-1}^{(r)}) \mathcal{P}(\sigma_{j'-1} | \overleftarrow{\sigma}_{j'-2}^{(r)}) \cdots \mathcal{P}(\sigma_{j'-n+1} | \overleftarrow{\sigma}_{j'-n}^{(r)}) \tag{14}$$

$$= \prod_{k=(j'-n+1)}^{j'} \mathcal{P}(\sigma_k | \overleftarrow{\sigma}_{k-1}^{(r)}) \tag{15}$$

where it suffices to know only the past r symbols for each transition under the r-Markovian assumption (Note: $s \geq r$). For any finite length adjacent symbol blocks $\overleftarrow{x}$, $\overleftarrow{y}$, and $\overleftarrow{z}$ in order, we have $\mathcal{P}(\overleftarrow{x} | \overleftarrow{y}\,\overleftarrow{z}) = \mathcal{P}(\overleftarrow{x}\,\overleftarrow{y} | \overleftarrow{y}\,\overleftarrow{z})$. Using this relation for each term in (12), setting $j' = n - 1$ without any loss of generality, and substituting the resulting expression in (12), the Hamiltonian is factored into a sum of transition energies as:

$$\mathcal{H} = -\sum_{k=0}^{n-1} \ln[\mathcal{P}(\overleftarrow{\sigma}_{k}^{(r)} | \overleftarrow{\sigma}_{k-1}^{(r)})] \quad \forall\, r \geq 1 \tag{16}$$

where the symbol blocks $\overleftarrow{\sigma}_{k}^{(r)} \equiv \sigma_k, \ldots, \sigma_{k-r+1} \equiv q_{\theta_k}^{[\ell]}$ and $\overleftarrow{\sigma}_{k-1}^{(r)} \equiv \sigma_{k-1}, \ldots, \sigma_{k-r} \equiv q_{\theta_{k-1}}^{[\ell]}$ belong to the set $\mathcal{Q}^{[\ell]}$ of ε-equivalence classes. An equivalent form of the Hamiltonian in (16) is expressed as:

$$\mathcal{H} = -\sum_{k=0}^{n-1} \ln[\mathcal{P}(q_{\theta_k}^{[\ell]} | q_{\theta_{k-1}}^{[\ell]})] = -\sum_{k=0}^{n-1} \mathcal{E}(q_{\theta_k}^{[\ell]} | q_{\theta_{k-1}}^{[\ell]}) \tag{17}$$

where the interaction energy associated with each term in (17) contributes to the total energy and depends only on the r nearest symbols in the past due to the Markov property. Therefore, the above construction is analogous to the effect of r nearest neighbor interactions in a lattice spin system, where the total energy is the sum of the interaction energies between spins and their (effective) neighbors. For a standard Markov process (i.e., $r = 1$), (16) reduces to:

$$\mathcal{H} = -\sum_{k=0}^{n-1} \ln[\mathcal{P}(\sigma_k | \sigma_{k-1})] \tag{18}$$

which is analogous to the structure of a generalized Ising model (GIM) with nearest neighbor interactions [13]. Furthermore, using general interaction energy functions in (9), a general form of the Hamiltonian in (16) is expressed as:

$$\mathcal{H} = -\sum_{k=0}^{n-1} \ln[\Phi(q_{\theta_k}^{[\ell]}, q_{\theta_{k-1}}^{[\ell]}) \mathcal{P}(q_{\theta_k}^{[\ell]} | q_{\theta_{k-1}}^{[\ell]})] = -\sum_{k=0}^{n-1} \mathcal{F}(q_{\theta_k}^{[\ell]} | q_{\theta_{k-1}}^{[\ell]}). \tag{19}$$

Equation (19) has the structure of a generalized Ising model (GIM) with r-nearest neighbor interactions on a renormalized symbol sequence. Each term is the interaction energy (see (9)) between a symbol block $q_{\theta_k}^{[\ell]} \equiv \overleftarrow{\sigma}_k^{(r)} \in \mathcal{Q}^{[\ell]}$ that is observed at time k and its preceding neighbor $q_{\theta_{k-1}}^{[\ell]} \equiv \overleftarrow{\sigma}_{k-1}^{(r)} \in \mathcal{Q}^{[\ell]}$ that is observed at time $k-1$. As time evolves, the symbol sequence makes transitions from one equivalence class to another and gives rise to different r-blocks.

Remark 3.3 Construction of the Hamiltonian in (19) is based on the assumption that the underlying process is a stationary r-Markov chain. In general, for dynamical systems, where the Markovian assumption is not valid, the above construction can be viewed as an approximation of the process dynamics by an r-Markov model. This approximation could lead to an inaccurate model of the underlying dynamics due to insufficient memory. On the other hand, representation of the process dynamics by a very large-order Markov model is undesirable because it would result in too many energy states. Having a large number of energy states would require a long observation sequence for frequency counting (see Appendix B) that may also lead to inaccuracy in the construction of transfer matrices for finite length sequences. Therefore, one alternative is renormalization that reduces the number of energy states by diminishing the effects of local dynamics.

On a renormalized symbol sequence, a procedure based on entropy rate is used for selection of r because increasing r beyond a certain value usually does not lead to any appreciable change in entropy; equivalently, the entropy rate would be very small. Given the current energy state, the entropy rate π of a symbolic stochastic process is defined as the uncertainty in the next symbol.

$$\pi = -\sum_{\theta=1}^{|\mathcal{Q}^{[\ell]}|} p_\theta \sum_{\varphi=1}^{|\Sigma^{[\ell]}|} \mathcal{P}(\sigma_\varphi | q_\theta^{[\ell]}) \log_2 \mathcal{P}(\sigma_\varphi | q_\theta^{[\ell]}) \tag{20}$$

where p_θ is the probability of occurrence of an energy state $q_\theta^{[\ell]}$; and $\mathcal{P}(\sigma_\varphi | q_\theta^{[\ell]})$ is the probability of occurrence of a symbol $\sigma_\varphi \in \Sigma^{[\ell]}$ at an energy state $q_\theta^{[\ell]}$. Being a measure of uncertainty, the entropy rate π in (20) monotonically decreases as r is increased. Beyond a certain point, increasing r is unlikely lead to any appreciable change in the entropy rate unless the process is heavily contaminated with white noise. This is the asymptotical entropy rate and the corresponding r is selected for the r-Markov approximation.

3.5 Transfer Matrix Approach for Pattern Identification

The analytical solution of one-dimensional spin systems with finite-range interactions is derived by expressing the partition function in terms of its finite-dimensional transfer matrix such that all thermodynamic information is encoded in the transfer matrix [1, 13]. The solution assumes cyclic periodic conditions, which are statistically justifiable for sufficiently large data sequences [1]. In terms of quasi-static equilibria in statistical mechanics, the effects of boundary conditions are negligible in the thermodynamic limit, i.e., when the length of the symbol sequence is sufficiently large (See Appendix B).

Definition 3.8 The partition function of a stationary r-Markov process is expressed as the sum of the exponentials of the energy of all physically admissible n-blocks over the n-block

space $\mathcal{B}^{(n)}$, such that

$$\mathcal{Z} \triangleq \sum_{\Gamma=1}^{|\mathcal{B}^{(n)}|} \exp(-\beta \mathcal{H}_\Gamma) \quad \text{for } n \gg r \geq 1 \tag{21}$$

where $\mathcal{H}_\Gamma$ is the Hamiltonian defined in (19); Γ is the index of a particular n-block in the block space $\mathcal{B}^{(n)}$; and $\beta > 0$ is a parameter that represents the inverse temperature under quasi-static equilibrium in the thermodynamic sense.

It follows from Definition 3.8 that the partition function represents the sum of energy exponentials of all possible symbol sequences of length n, i.e., an ensemble of n-blocks. Since the transition probabilities between energy states are calculated from the symbol sequence that is generated from time series data of measurements, the contribution of each possible n-block towards the partition function is different. Therefore, the n-blocks that have lower energies given by the corresponding Hamiltonians contribute more heavily to the partition function as compared to n-blocks that have higher energies (see (21)).

It follows from (19) and (21) that:

$$\mathcal{Z} = \sum_{\Gamma=1}^{|\mathcal{B}^{(n)}|} \exp\left(\beta \sum_{k=0}^{n-1} \ln[\Phi(q_{\theta_k}^{[\ell]}, q_{\theta_{k-1}}^{[\ell]}) \mathcal{P}(q_{\theta_k}^{[\ell]} | q_{\theta_{k-1}}^{[\ell]})]\right) \tag{22}$$

$$= \sum_{\Gamma=1}^{|\mathcal{B}^{(n)}|} \exp\left(\sum_{k=0}^{n-1} \ln[\Phi^\beta(q_{\theta_k}^{[\ell]}, q_{\theta_{k-1}}^{[\ell]}) \mathcal{P}^\beta(q_{\theta_k}^{[\ell]} | q_{\theta_{k-1}}^{[\ell]})]\right) \tag{23}$$

$$= \sum_{\Gamma=1}^{|\mathcal{B}^{(n)}|} \prod_{k=0}^{n-1} (\Phi^\beta(q_{\theta_k}^{[\ell]}, q_{\theta_{k-1}}^{[\ell]}) \mathcal{P}^\beta(q_{\theta_k}^{[\ell]} | q_{\theta_{k-1}}^{[\ell]})) \tag{24}$$

$$= \sum_{\Gamma=1}^{|\mathcal{B}^{(n)}|} \prod_{k=0}^{n-1} \mathcal{T}_{q_{\theta_k}^{[\ell]}, q_{\theta_{k-1}}^{[\ell]}} \tag{25}$$

where $\mathcal{T}_{q_{\theta_k}^{[\ell]}, q_{\theta_{k-1}}^{[\ell]}} \triangleq \Phi^\beta(q_{\theta_k}^{[\ell]}, q_{\theta_{k-1}}^{[\ell]}) \mathcal{P}^\beta(q_{\theta_k}^{[\ell]} | q_{\theta_{k-1}}^{[\ell]})$. Since all pairs $q_{\theta_k}^{[\ell]} \in \mathcal{Q}^{[\ell]}$ and $q_{\theta_{k-1}}^{[\ell]} \in \mathcal{Q}^{[\ell]}$ in (25) can (possibly) have at most $|\mathcal{Q}^{[\ell]}|$ configurations, a $|\mathcal{Q}^{[\ell]}| \times |\mathcal{Q}^{[\ell]}|$ non-negative transfer matrix $\mathcal{T}$ [13] is constructed as:

$$\mathcal{T} \triangleq \left[\mathcal{T}\right]_{\varphi\theta} = \Phi^\beta(q_\varphi^{[\ell]}, q_\theta^{[\ell]}) \mathcal{P}^\beta(q_\varphi^{[\ell]} | q_\theta^{[\ell]}) \quad \text{for } \theta, \varphi \in \{0, 1, \ldots, |\mathcal{Q}^{[\ell]}| - 1\} \tag{26}$$

where both $q_\theta^{[\ell]}$ and $q_\varphi^{[\ell]}$ belong to $\mathcal{Q}^{[\ell]}$ and denote the respective energy states (i.e., ε-equivalence classes) generated from the renormalized sequence. Since the summation in (25) is taken over all possible blocks in $\mathcal{B}^{(n)}$, the transfer matrix in (26) is constructed to include interactions between all ε-equivalence classes. The transfer matrix $\mathcal{T}$ encodes more information about the statistical characteristics of the dynamical system than the scalar valued partition function $\mathcal{Z}$. It follows from Eq. (25) that $\mathcal{Z}$ is trace of the $|\mathcal{Q}^{[\ell]}| \times |\mathcal{Q}^{[\ell]}|$ non-negative matrix $(\mathcal{T})^n$ [1, 13]. As an illustrative example, let $\Sigma^{[\ell]} = \{0, 1\}$ be the alphabet and let the interaction range be $r = 2$. Then, the total number of (possible) equivalence classes is $|\mathcal{Q}^{[\ell]}| = 4$, where $\mathcal{Q}^{[\ell]} = \{\overleftarrow{00}, \overleftarrow{10}, \overleftarrow{01}, \overleftarrow{11}\}$. The $|\mathcal{Q}^{[\ell]}| \times |\mathcal{Q}^{[\ell]}|$ transfer matrix for

this example is shown below:

$$\mathcal{T} = \begin{pmatrix} \mathcal{T}_{\overleftarrow{00},\overleftarrow{00}} & \mathcal{T}_{\overleftarrow{10},\overleftarrow{00}} & \mathcal{T}_{\overleftarrow{01},\overleftarrow{00}} & \mathcal{T}_{\overleftarrow{11},\overleftarrow{00}} \\ \mathcal{T}_{\overleftarrow{00},\overleftarrow{10}} & \mathcal{T}_{\overleftarrow{10},\overleftarrow{10}} & \mathcal{T}_{\overleftarrow{01},\overleftarrow{10}} & \mathcal{T}_{\overleftarrow{11},\overleftarrow{10}} \\ \mathcal{T}_{\overleftarrow{00},\overleftarrow{01}} & \mathcal{T}_{\overleftarrow{10},\overleftarrow{01}} & \mathcal{T}_{\overleftarrow{01},\overleftarrow{01}} & \mathcal{T}_{\overleftarrow{11},\overleftarrow{01}} \\ \mathcal{T}_{\overleftarrow{00},\overleftarrow{11}} & \mathcal{T}_{\overleftarrow{10},\overleftarrow{11}} & \mathcal{T}_{\overleftarrow{01},\overleftarrow{11}} & \mathcal{T}_{\overleftarrow{11},\overleftarrow{11}} \end{pmatrix}.$$

For $\ell = 0$, $q_\theta^{[0]} \equiv q_\theta \in \mathcal{Q}$ and $q_\varphi^{[0]} \equiv q_\varphi \in \mathcal{Q}$ represent ε-equivalence classes generated from the original sequence without the block symbol transformation and the transfer matrix $\mathcal{T}$ reduces to the original $|\mathcal{Q}| \times |\mathcal{Q}|$ matrix.

For dynamical systems, the inverse temperature $\beta \sim 1/T$ in (26) plays the role of a sensitivity parameter [13]. If $\beta \to 0$, the temperature T tends to ∞ in the thermodynamic sense, implying that the increase in randomness would render all permissible transitions to be equally probable in the transfer matrix $\mathcal{T}$. This phenomenon leads to maximum uncertainty and the information content obtained from $\mathcal{T}$ is minimized. On the contrary, as β is increased, the temperature T of the system decreases; consequently, the uncertainty is reduced and more information and new facets of the system are revealed; however, if β becomes too large (i.e., the temperature approaches absolute zero in the thermodynamic sense), the most relevant information tends to mask other information and this is also undesirable. The parameter β can scan the structure of the transfer matrix $\mathcal{T}$. Therefore, the transfer matrix $\mathcal{T}$ can be adjusted with an appropriate choice of the parameter β based on the desired sensitivity. If all transitions are assigned equal strength, then setting $\beta = 1$ reduces the transfer matrix $\mathcal{T}$ to a transition matrix that consists of the probabilities of all possible transitions between different energy states.

3.5.1 Calculation of the Transfer Matrix for Pattern Identification

The construction of transfer matrix $\mathcal{T}$ requires calculation of the transition probabilities between all energy states (i.e., ε-equivalence classes) in set $\mathcal{Q}^{[\ell]}$ (see (26)). The transition probabilities can be calculated based on the principle of sliding block codes [22]. An energy state $q_\theta^{[\ell]} \in \mathcal{Q}^{[\ell]}$ changes to another energy state $q_\varphi^{[\ell]} \in \mathcal{Q}^{[\ell]}$ upon occurrence of a symbol $\sigma \in \Sigma^{[\ell]}$. On a given symbol sequence (possibly renormalized, i.e., $\ell > 0$), a window of length r is shifted to the left (i.e., forward time direction) by one symbol at a time, such that it retains the last $(r-1)$ symbols of the previous window and appends the new symbol at the tip. The symbolic permutation of length r in the current window gives rise to a new energy state. The counts of occurrences of word sequences $\sigma q_\theta^{[\ell]}$ and $q_\theta^{[\ell]}$ are kept that are respectively denoted by $N(\sigma q_\theta^{[\ell]})$ and $N(q_\theta^{[\ell]})$. Note that if $N(q_\theta^{[\ell]}) = 0$, then the energy state $q_\theta^{[\ell]} \in \mathcal{Q}^{[\ell]}$ has zero probability of occurrence. For $N(q_\theta^{[\ell]}) > 0$, the transitions probabilities are obtained by these frequency counts as follows:

$$\mathcal{P}(q_\varphi^{[\ell]}|q_\theta^{[\ell]}) \equiv \frac{\mathcal{P}(q_\varphi^{[\ell]},\ q_\theta^{[\ell]})}{\mathcal{P}(q_\theta^{[\ell]})} = \frac{\mathcal{P}(\sigma q_\theta^{[\ell]})}{\mathcal{P}(q_\theta^{[\ell]})} \Rightarrow \mathcal{P}(q_\varphi^{[\ell]}|q_\theta^{[\ell]}) \approx \frac{N(\sigma q_\theta^{[\ell]})}{N(q_\theta^{[\ell]})}. \tag{27}$$

For implementation purposes, the state transition probabilities can be calculated via construction of a probabilistic finite state automata (PFSA) [42], whose states are the energy states (i.e., the ε-equivalence classes) and the edges denote the transitions from one energy state to the other upon occurrence of a new symbol. Therefore, the arc probabilities of the

PFSA represent the transition probabilities between different energy states, which are generated from a symbol sequence over the PFSA. Once the transition probabilities are obtained, the elements of the transfer matrix are calculated via (26). The information content in the transfer matrix depends on the block symbol transformation of the original symbol sequence generated from the observed time series data and the interaction range r between symbols on the renormalized sequence.

Remark 3.4 In general, the generalized Ising models (GIMs) can be constructed from a diverse range of block symbol transformations via different block widths w and shifts χ. Higher block symbol transformations reveal coarser dynamics of the system. Furthermore, the interaction range r can be varied to generate a diverse range of interactions. Such GIMs can be constructed in a hierarchical structure to provide rich information on the underlying dynamics of the complex system.

The transfer matrix $\mathcal{T}$ is calculated from the (fast scale) symbol sequences at different slow-time epochs $t_{s_0}, t_{s_1}, \ldots, t_{s_n}$. The renormalized symbol sequence obtained from the observed time series data under the reference condition (e.g., time epoch t_{s_0}) generates the transfer matrix $\mathcal{T}^{ref}$. At subsequent slow-time epochs, $t_{s_1}, t_{s_2}, \ldots, t_{s_n}$, symbol sequences are generated from the corresponding time series data sets, that, in turn, are used to generate the transfer matrices $\mathcal{T}^{s_1}, \mathcal{T}^{s_2}, \ldots, \mathcal{T}^{s_n}$, respectively. The partitioning is kept invariant as that of the reference condition at the time epoch t_{s_0}. If the quasi-stationary dynamics of the system change (possibly due to growth of anomalies) on the slow scale, the goal is to identify these changes from the statistical patterns of the observed symbol sequences. Therefore, the evolution of $\mathcal{T}$ on a slow scale with respect to the nominal condition (i.e., time epoch t_{s_0}) represents the gradual growth of (parametric or non-parametric) changes in the dynamical system. For pattern identification, the transfer matrix $\mathcal{T}$ is converted to a stochastic matrix $\mathcal{U}$ by unity sum-normalization of its rows using the following transformation:

$$\mathcal{U} = \mathcal{D}\mathcal{T} \tag{28}$$

where D is a diagonal matrix, such that $D_{\theta,\theta} = 1/\sum_{\varphi=1}^{|\mathcal{Q}^{[\ell]}|} \mathcal{T}_{\varphi,\theta}$ for $\theta = 1, \ldots, |\mathcal{Q}^{[\ell]}|$. The left eigenvector $\mathbf{p}$, called the *pattern vector*, is obtained corresponding to the (unique) unit eigenvalue of the (irreducible) stochastic matrix $\mathcal{U}$ [43]. The generated pattern vectors are robust to measurement noise and spurious disturbances, because transformation of the raw signal to symbol sequences (see Sect. 3.1) attenuates noise via signal preprocessing and coarse graining of the data. Furthermore, the statistical analysis to generate the pattern vectors eliminates infrequent disturbances.

3.5.2 Calculation of a Macroscopic Parameter

Behavioral pattern changes, if any, are detected at time epoch t_{s_j} with respect to the reference condition at t_{s_0} by defining a macroscopic scalar parameter ψ, such that

$$\psi^{s_j} = f(\mathbf{p}^{s_j}, \mathbf{p}^{s_{j-1}}, \ldots, \mathbf{p}^{ref}) \tag{29}$$

where $f(\bullet, \bullet, \ldots, \bullet)$ is a path function of the evolution of the pattern vector $\mathbf{p}$ on the slow scale, where $\mathbf{p}^{s_j}$ and $\mathbf{p}^{ref}$ are pattern vectors generated from the irreducible stochastic matrices $\mathcal{U}^{s_j}$ and $\mathcal{U}^{ref}$, respectively. Another choice of a macroscopic parameter ψ is a relative function $d(\mathbf{p}^{s_j}, \mathbf{p}^{ref})$ that defines a distance (e.g., the standard Euclidean norm, the L_1 norm,

and Kullback distance [44]) between the pattern vector $\mathbf{p}^{s_j}$ and the nominal pattern vector $\mathbf{p}^{ref}$. In general, an analytical variable derived from the statistical pattern vectors can serve as a macroscopic parameter for dynamical systems and can be chosen based on desired sensitivity related to the particular application.

4 Experimental Validation of the Pattern Identification Algorithm

This section presents experimental validation of the pattern identification concept on a laboratory apparatus for real-time monitoring of the effects of evolving microstructural changes in polycrystalline alloys based on in situ ultrasonic sensing [45, 46]. In the current state-of-the-art, no existing model, solely based on the fundamental principles of physics [1], can adequately capture the dynamical behavior of fatigue damage at the grain level. Although microstructural damage can be qualitatively assessed by electron microscopy, there exists no precise method for real-time quantitative evaluation of gradually evolving microstructural changes relative to the nominal (i.e., reference) condition. This section presents some of the experimental results generated from the observed ultrasonic data.

The test apparatus is loaded with a specimen of 7075-T6 aluminum alloy that is subjected to tensile-tensile cyclic loading at 12 Hz with the maximum and minimum load amplitudes of 85 MPa and 4.85 MPa under the regulation of computer-controlled electro-hydraulic servo-valves [47]. The specimen is 3 mm thick and 50 mm wide, and has a semi-circular notch of 1.58 mm $\times$ 4.7 mm one side. A piezoelectric transducer is used to inject 10 MHz ultrasonic waves in a specimen and a receiver transducer is placed on the other side of notch to measure the transmitted signal after it has traveled through the region of microstructural damage. Similar to the propagation of any wave, discontinuities in the propagation medium of ultrasonic waves cause additive and destructive interference. Since material characteristics (e.g., voids, dislocations and short cracks) influence ultrasonic impedance, a small irregularity in the specimen is likely to change the signature of the signal at the receiver end. Since ultrasonic waves have a very small wavelength (relative to the dimension of microstructural flaws), very small irregularities can be detected. Therefore, the received signal can be used to capture minute details and small changes during the early stages of fatigue damage, which may not possible to detect by an optical microscope.

For data acquisition, the slow time epochs were chosen to be 1000 load cycles (i.e., $\sim$80 s) apart and a string of 10,000 data points was collected at every slow time epoch. The nominal condition at the slow time epoch t_{s0} was chosen to be $\sim$ 1 kilocycle to ensure that the electro-hydraulic system of the test apparatus had come to a steady state. Following the pattern identification algorithm, the ultrasonic data was transformed to a symbol sequence using the Analytic-signal-space partitioning (*ASSP*) [37] based on the maximum entropy principle [36] with an alphabet size of $|\Sigma| = 8$. Following Sect. 3.3, the symbol sequence was renormalized by setting $\chi = w = 2$ (i.e., a higher power shift). A block of width w was assigned the symbol that corresponds to the higher element of the partition as the new block symbol such that $\Sigma^{[1]} = \Sigma$. The nearest-neighbor (i.e., $r = 1$) interactions were considered for generation of the transfer matrix and β was chosen to be equal to one. Furthermore, unity strength was assigned to each state transition. With this selection, the pattern identification tool was able to capture the anomalies significantly earlier than through usage of the in-situ traveling optical microscope. Increasing the value of $|\Sigma|$ further did not improve the results and increasing the value of r created a large number of energy states, many of these states having very small or zero probabilities. The advantage of having a small number of energy states is fast computation on an inexpensive processor as well as robustness to noise and spurious disturbances.

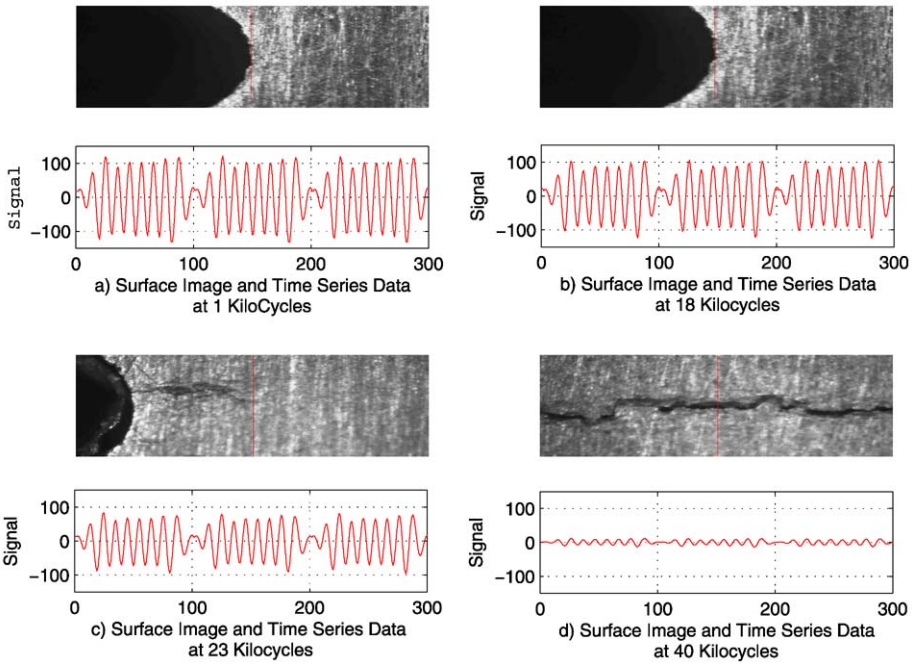

Fig. 6 An example of damage evolution in mechanical systems and measurement using ultrasonic signals

The evolution of fatigue damage is exhibited at different slow time epochs in Fig. 6 that shows four pairs of plots from (a) to (d). In each pair, the top plot displays the surface image of the test specimen, as seen by the optical microscope at a certain time epoch; and the bottom plot displays the (processed) ultrasonic time series data collected at the corresponding time epoch. (Note: Only 300 data points are shown in each image, however, the actual data string consists of 10,000 points that was used for analysis at each slow time epoch.) The image in Fig. 6(a) shows the nominal condition at ∼1 kilocycle when there is negligible damage in the specimen. The image in Fig. 6(b) shows the specimen surface at 18 kilocycles before the appearance of crack on the surface. Apparently, this image does not yet have any indication of surface crack although the corresponding bottom plate does exhibit a deviation from the ultrasonic data at the nominal condition in Fig. 6(a). The image in Fig. 6(c) exhibits noticeable appearance of a crack on the specimen surface at 23 kilocycles, which is often considered as the boundary of crack initiation and crack propagation phases in the fracture mechanics literature [21]. The appearance of a large surface crack indicates that a significant portion of the crack or multiple small cracks might have already developed underneath the surface before they started spreading on the surface. At the onset of the crack propagation phase, the fatigue damage progresses relatively faster and shows rapid development of a large crack. The image in Fig. 6(d) exhibits a fully developed crack at 40 kilocycles. The corresponding bottom plate shows the ultrasonic data that is almost zero due to complete attenuation.

Figure 7 shows the evolution of the macroscopic parameter that is generated from (29) by analyzing the ultrasonic data sets at different slow time epochs. The function f in (29) was chosen to be a cumulative sum of the incremental damage measured by the Euclidean distance between adjacent pattern vectors [45]. A sharp change in the slope of the macroscopic

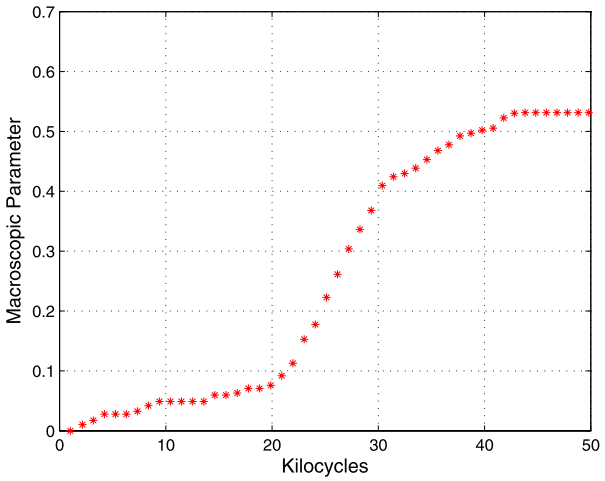

Fig. 7 Evolution of the macroscopic parameter

parameter indicates the onset of crack propagation phase, which occurs upon appearance of a surface crack at ∼23 kilocycles and could be perceived as a first-order phase transition [40]. (Note: the notion of equilibrium statistical mechanics does not hold for phase transitions.) It is observed that small changes can be detected significantly before the optical microscope can capture a surface crack. The slope of the anomaly measure represents the damage growth rate while the magnitude indicates the accumulated fatigue damage starting from the nominal condition. The critical information lies in the crack initiation phase where no crack was visible on the surface. This is the region where microstructural damage such as multiple small cracks possibly caused small changes in the ultrasonic signal profile. In the crack propagation phase the macroscopic parameter shows a significantly faster growth as compared to the slow growth during crack initiation.

5 Summary, Conclusions, and Recommendations for Future Work

The paper presents a theoretical concept of data-driven pattern identification in dynamical systems based on the principles of statistical mechanics. Potentially, this concept of pattern identification is of paramount importance to diverse disciplines (e.g., electromechanical, aerospace, sensor network, environmental, biological, and sociological systems) related to applied physics and engineering science. These dynamical systems may gradually evolve over a slow time scale until occurrence of major disruptions. The nominal behavior of such dynamical systems are assumed to follow the laws of equilibrium thermodynamics and the disruptive conditions (e.g., onset of chaos in the vicinity of bifurcation) could be perceived to be analogous to phase transitions and other forms of non-equilibrium thermodynamics. While large disruptions are usually conspicuous, this paper addresses identification of gradually evolving patterns in complex systems.

Analytical relationships have been formulated to construct analogies between the concepts of statistical mechanics and symbolic dynamics for pattern identification. The underlying theory is formulated to construct macroscopic patterns from symbol sequences that are generated from observed time series data. In particular, the concepts of lattice spin systems

are used for construction of pattern identification algorithms based on transfer matrix analysis of the generalized Ising model (GIM) of a symbol sequence. These algorithms include coarser representations of the dynamical system via block symbol transformations of the original system for reduced complexity. Pertinent results are experimentally validated on a computer-controlled and richly instrumented laboratory apparatus under oscillating load for behavior pattern changes due to gradual evolution of fatigue damage in a polycrystalline alloy.

Further theoretical, computational, and experimental research is necessary before the concepts, presented in this paper, can be applied to real-life environments. Specifically, the following research areas are recommended as topics of future work.

- Extension of one-dimensional spin system models to multidimensional spin system models for data fusion and pattern identification in multidimensional data sets (e.g., two-dimensional images).
- Extension of the pattern identification method in non-stationary signals using the concepts of non-equilibrium statistical mechanics.
- Pattern identification of global behavioral changes in large-scale multi-agent systems (e.g., sensor networks and robot swarms).
- Application of the Renormalization Group theory for identification of (first and higher order) phase transitions and the associated critical phenomena in complex dynamical systems.
- Selection of an appropriate order parameter (i.e, the macroscopic variable) based on the desired sensitivity of change detection.

Acknowledgements The authors would like to thank the anonymous reviewers whose thoughtful comments and suggestions have improved the quality of the paper.

Appendix A: Sliding Block Codes

The shift space formalism is a systematic way to study the properties of dynamical systems encoded through symbolic dynamics. The different shift spaces provide increasingly powerful classes of models that can be used to generate statistical patterns for behavior identification in complex systems as presented in this paper.

Definition A.1 Let Σ be a (finite) alphabet. The *full* Σ*-shift* is the collection of all bi-infinite sequences of symbols from Σ and is denoted by:

$$\Sigma^{\mathbb{Z}} = \{\upsilon = \{\upsilon_i\}_{i\in\mathbb{Z}} : \upsilon_i \in \Sigma \ \forall i \in \mathbb{Z}\}. \tag{30}$$

Definition A.2 The *shift map* ζ on the full shift $\Sigma^{\mathbb{Z}}$ maps a point υ to a point $\tau = \zeta(\upsilon)$ whose ith coordinate is $\tau_i = \upsilon_{i+1}$.

A block is a finite sequence of symbols over Σ. Let $\upsilon \in \Sigma^{\mathbb{Z}}$ and b be a block over Σ. Then b occurs in υ if there exists indices i and j such that $b = \upsilon_{[j,i]} = \upsilon_j \upsilon_{j-1} \cdots \upsilon_i$. Note that the empty block ϵ occurs in every υ.

Definition A.3 Let F be a collection of blocks, i.e., (finite) sequences of symbols over Σ. For any such F, let us define X_F to be the subset of sequences in $\Sigma^{\mathbb{Z}}$, which do not contain any block in F. A *shift space* is a subset X of a full shift $\Sigma^{\mathbb{Z}}$ such that $X = X_F$ for some collection F of forbidden blocks over Σ.

For a given shift space, the collection F is at most countable (i.e., finite or countably infinite) and is non-unique (i.e., there may be many such F's describing the shift space). As subshifts of full shifts, these spaces share a common feature called *shift invariance*. Since the constraints on points are given in terms of forbidden blocks alone and do not involve the coordinate at which a block might be forbidden, it follows that if $\upsilon \in X_F$, then so are its shifts $\zeta(\upsilon)$ and $\zeta^{-1}(\upsilon)$. Therefore, $\zeta(X_F) = X_F$, which is a necessary condition for a subset of Σ^Z to be a shift space. This property introduces the concept of shift dynamical systems.

Definition A.4 Let X be a shift space and $\zeta_X : X \to X$ be the shift map. Then (X, ζ_X) is known as a *shift dynamical system*.

The shift dynamical system mirrors the dynamics of the original dynamical system from which it is generated (by symbolic dynamics). Several examples of shift spaces are given in [22]. Rather than describing a shift space by specifying the forbidden blocks, it can also be specified by allowed blocks.

Definition A.5 Let X be a subset of a full shift, and let $\mathcal{B}^{(n)}(X)$ denote the set of all n-blocks (i.e., blocks of length n) that occur in X. The language of the shift space X is defined by block space $\mathcal{B}(X)$ as:

$$\mathcal{B}(X) = \bigcup_{n=0}^{\infty} \mathcal{B}^{(n)}(X). \tag{31}$$

Sliding Block Codes Let X be a shift space over the alphabet Σ, then $\upsilon \in X$ can be transformed into a new sequence $\upsilon' = \cdots \upsilon'_1 \upsilon'_{-1} \upsilon'_0 \cdots$ over another alphabet Σ' as follows. Fix integers m and n such that $-m \leq n$. To compute υ'_i of the transformed sequence, we use a function Ψ that depends on the "window" of coordinates of υ from $i - m$ to $i + n$. Here, $\Psi : \mathcal{B}^{(m+n+1)}(X) \to \Sigma'$ is a fixed *block map*, called a $(m + n + 1)$-*block map*, from the allowed $(m + n + 1)$-blocks in X to symbols in Σ'. Therefore,

$$\upsilon'_i = \Psi(\upsilon_{i+n} \cdots \upsilon_{i-m+1} \upsilon_{i-m}) = \Psi(\upsilon_{[i+n, i-m]}). \tag{32}$$

Definition A.6 Let Ψ be a block map as defined in (32). Then the map $\psi : X \to (\Sigma')^{\mathbb{Z}}$ defined by $\upsilon' = \psi(\upsilon)$ with υ'_i given by (32) is called the *sliding block code* induced by Ψ with memory m and anticipation n.

Definition A.7 Let X and Y be shift spaces, and $\psi : X \to Y$ be a sliding block code.

- If $\psi : X \to Y$ is onto, then ϕ is called a *factor code* from X onto Y.
- If $\psi : X \to Y$ is one-to-one, then ϕ is called an *embedding* of X into Y.
- If $\psi : X \to Y$ has a inverse (i.e., there exists a sliding block code $\phi : Y \to X$ such that $\phi(\psi(\upsilon)) = \upsilon \ \ \forall \upsilon \in X$ and $\phi(\psi(\gamma)) = \gamma \ \forall \ \gamma \in Y$), then ψ is called a *conjugacy* from X to Y.

If there exists a conjugacy from X to Y, then Y can be viewed as a copy of X, sharing all properties of X. Therefore, a conjugacy is often called topological conjugacy in literature [22].

Appendix B: Stopping Rule for Determining Symbol Sequence Length

This section presents a stopping rule that is necessary to find a lower bound on the length of symbol sequences required for parameter identification of the state transition matrix Π that is equal to the transfer matrix $\mathcal{T}$ for uniform strengths and for $\beta = 1$. The idea is to have sufficiently large symbol sequence such that the state transition matrix Π is saturated. The stopping rule [48] is based on the properties of irreducible stochastic matrices [43]. The state transition matrix is constructed at the λ iteration step (i.e., from a symbol sequence of length λ) as $\Pi(\lambda)$ that is an $m \times m$ irreducible stochastic matrix under stationary conditions. Similarly, the state probability vector $\mathbf{p}(\lambda) \equiv [p_1(\lambda)\ p_2(\lambda)\ \cdots\ p_m(\lambda)]$ is obtained as

$$p_i(\lambda) = \frac{\lambda_i}{\sum_{j=1}^{m} \lambda_i} \tag{33}$$

where λ_i is the number of r-blocks representing the ith equivalence class such that $\left(\sum_{j=1}^{m} \lambda_j\right) + r - 1 = \lambda$ is the total length of the data sequence under symbolization.

The stopping rule makes use of the Perron-Frobenius Theorem [43] to establish a relation between the vector $\mathbf{p}(\lambda)$ and the matrix $\Pi(\lambda)$. Since the matrix $\Pi(\lambda)$ is stochastic and irreducible, there exists a unique unit eigenvalue and the corresponding left eigenvector $\mathbf{p}(\lambda)$ (normalized to unity in the sense of absolute sum). The left eigenvector $\mathbf{p}(\lambda)$ represents the probability vector, provided that the matrix parameters have converged after a sufficiently large number of iterations. That is,

$$\mathbf{p}(\lambda) = \mathbf{p}(\lambda)\Pi(\lambda) \quad \text{as } \lambda \to \infty. \tag{34}$$

Following (33), the absolute error between successive iterations is obtained such that

$$\|(\mathbf{p}(\lambda) - \mathbf{p}(\lambda + 1))\|_\infty = \|\mathbf{p}(\lambda)(\mathbf{I} - \Pi(\lambda))\|_\infty \leq \frac{1}{\lambda} \tag{35}$$

where $\| \bullet \|_\infty$ is the max norm of the finite-dimensional vector $\bullet$.

To calculate the stopping point λ_s, a tolerance of η $(0 < \eta \ll 1)$ is specified for the relative error such that:

$$\frac{\|(\mathbf{p}(\lambda) - \mathbf{p}(\lambda + 1))\|_\infty}{\|(\mathbf{p}(\lambda))\|_\infty} \leq \eta \quad \forall\, \lambda \geq \lambda_s. \tag{36}$$

The objective is to obtain the least conservative estimate for λ_s such that the dominant elements of the probability vector have smaller relative errors than the remaining elements. Since the minimum possible value of $\|(\mathbf{p}(\lambda))\|_\infty$ for all λ is $\frac{1}{m}$, where m is the dimension of $\mathbf{p}(\lambda)$, the best worst case value of the stopping point is obtained from (35) and (36) as:

$$\lambda_s \equiv \text{int}\left(\frac{m}{\eta}\right) \tag{37}$$

where int$(\bullet)$ is the integer part of the real number $\bullet$.

References

1. Pathria, R.K.: Statistical Mechanics. Elsevier Science and Technology Books, Amsterdam (1996)

2. Bellouquid, A., Delitala, M.: Mathematical Modeling of Complex Biological Systems: A Kinetic Theory Approach (Modeling and Simulation in Science, Engineering and Technology). Birkhäuser, Boston (2006)
3. Dill, K.A., Lucas, A., Hockenmaier, J., Huang, L., Chiang, D., Joshi, A.K.: Computational linguistics: A new tool for exploring biopolymer structures and statistical mechanics. Polymer **48**, 4289–4300 (2007)
4. Blossey, R.: Computational Biology: A Statistical Mechanics Perspective. Mathematical and Computational Biology Series, vol. 12, Chapman and Hall/CRC, Boca Raton (2006)
5. Martino, A.D., Marsili, M.: Statistical mechanics of socio-economic systems with heterogeneous agents. J. Phys. A: Math. Gen. **39**(43), R465–R540 (2006)
6. Stanley, H.E., Gabaix, X., Gopikrishnan, P., Plerou, V.: Economic fluctuations and statistical physics: the puzzle of large fluctuations. Nonlinear Dyn. **44**(1–4), 329–340 (2006)
7. Maurer, B.A.: Statistical mechanics of complex ecological aggregates. Ecol. Complex. **2**(1), 71–85 (2005)
8. Albert, R., Barabasi, A.: Statistical mechanics of complex networks. Rev. Mod. Phys. **74**(1), 47–97 (2002)
9. Dorogovtsev, S.N., Goltsev, A.V., Mendes, J.E.F.: Critical phenomena in complex networks, arXiv:0705.0010v2 [cond-mat.stat-mech] (2007)
10. Satorras, R.P., Rubi, J.M., Guilera, A.D.: Statistical Mechanics of Complex Networks. Springer, New York (2003)
11. Ruelle, D.: Thermodynamic Formalism. Cambridge University Press, Cambridge (2004)
12. Badii, R., Politi, A.: Complexity Hierarchical Structures and Scaling in Physics. Cambridge University Press, Cambridge (1997)
13. Beck, C., Schlögl, F.: Thermodynamics of Chaotic Systems: An Introduction. Cambridge University Press, Cambridge (1993)
14. Ott, E.: Chaos in Dynamical Systems. Cambridge University Press, Cambridge (2003)
15. Ray, A.: Symbolic dynamic analysis of complex systems for anomaly detection. Signal Process. **84**(7), 1115–1130 (2004)
16. Klesnil, M., Lukas, P.: Fatigue of Metallic Materials, 71st edn. Material Science Monographs. Elsevier, Amsterdam (1991)
17. Kantz, H., Schreiber, T.: Nonlinear Time Series Analysis, 2nd edn. Cambridge University Press, Cambridge (2004)
18. Shannon, C.E.: A mathematical theory of communications. Bell Syst. Tech. J. **27**, 379–423 (1948)
19. Eckmann, J.P., Ruelle, D.: Ergodic theory of chaos and strange attractors. Rev. Mod. Phys. **57**3(I)
20. Olemskoi, A., Kokhan, S.: Effective temperature of self-similar time series: analytical and numerical developments. Physica A: Stat. Mech. Appl. **360**(1), 37–58 (2006)
21. Gupta, S., Ray, A.: Pattern identification using lattice spin systems: a thermodynamic formalism. Appl. Phys. Lett. **91**(19), 194105 (2007)
22. Lind, D., Marcus, M.: An Introduction to Symbolic Dynamics and Coding. Cambridge University Press, Cambridge (1995)
23. Buhl, M., Kennel, M.: Statistically relaxing to generating partitions for observed time-series data. Phys. Rev. E **71**(4), 046213 (2005)
24. Feldman, D.P.: Computational mechanics of classical spin systems. PhD thesis, Department of Physics, University of California Davis (1998)
25. Martin, P.: Potts Models and Related Problems in Statistical Mechanics. World Scientific, Singapore (1991)
26. Potts, R.B.: Some generalized order–disorder transformations. Proc. Camb. Philos. Soc. **48**, 106–109 (1952)
27. Wu, F.Y.: The Potts model. Rev. Mod. Phys. **54**(1), 235–268 (1982)
28. Dobson, J.F.: Many-neighbored Ising chain. J. Math. Phys. **10**(1), 40–45 (1969)
29. Ising, E.: Z. Phys. **21**, 613 (1925)
30. Huang, K.: Statistical Mechanics. Wiley, New York (1987)
31. Duda, R., Hart, P., Stork, D.: Pattern Classification. Wiley, New York (2001)
32. Daw, C.S., Finney, C.E.A., Tracy, E.R.: A review of symbolic analysis of experimental data. Rev. Sci. Instrum. **74**(2), 915–930 (2003)
33. Gupta, S., Ray, A.: Symbolic dynamic filtering for data-driven pattern recognition. In: Zoeller, E.A. (ed.) Pattern Recognition: Theory and Application. Nova Science, New York (2008), Chap. 2
34. Gupta, S., Ray, A., Keller, E.: Symbolic time series analysis of ultrasonic data for early detection of fatigue damage. Mech. Syst. Signal Process. **21**(2), 866–884 (2007)
35. Mallat, S.: A Wavelet Tour of Signal Processing, 2nd edn. Academic Press, New York (1998)

36. Rajagopalan, V., Ray, A.: Symbolic time series analysis via wavelet-based partitioning. Signal Process. **86**(11), 3309–3320 (2006)
37. Subbu, A., Ray, A.: Space partitioning via Hilbert transform for symbolic time series analysis. Appl. Phys. Lett. **92**, 084107 (2008)
38. Cover, T.M., Thomas, J.A.: Elements of Information Theory. Wiley, New York (1991)
39. Rudin, W.: Real Complex Analysis, 3rd edn. McGraw Hill, New York (1988)
40. Goldenfeld, N.: Lectures on Phase Transitions and the Renormalization Group. Perseus Books, Reading (1992)
41. Peng, S.: Order isomorphism under higher power shift and generic form of renormalization group equations in multimodal maps. Chaos Solitons Fractals **23**, 1757–1775 (2005)
42. Hopcroft, H.E., Motwani, R., Ullman, J.D.: Introduction to Automata Theory, Languages, and Computation, 2nd edn. Addison Wesley, Boston (2001)
43. Bapat, R.B., Raghavan, T.E.S.: Nonnegative Matrices and Applications. Cambridge University Press, Cambridge (1997)
44. Naylor, A.W., Sell, G.R.: Linear Operator Theory in Engineering and Science. Springer, New York (1982)
45. Gupta, S., Ray, A., Keller, E.: Symbolic time series analysis of ultrasonic signals for fatigue damage monitoring in polycrystalline alloys. Meas. Sci. Technol. **17**(7), 1963–1973 (2006)
46. Gupta, S., Ray, A.: Real-time fatigue life estimation in mechanical systems. Meas. Sci. Technol. **18**(7), 1947–1957 (2007)
47. Keller, E.E., Ray, A.: Real time health monitoring of mechanical structures. Struct. Health Monit. **2**(3), 191–203 (2003)
48. Ray, A.: Signed real measure of regular languages for discrete-event supervisory control. Int. J. Control **78**(12), 949–967 (2005)